Available online at www.sciencedirect.com
ScienceDirect
Thin Solid Films 516 (2008) 5118–5121
www.elsevier.com/locate/tsf

Spatially-resolved photocapacitance measurements to study defects in a-Si:H based p–i–n particle detectors

C. Casteleiro [a], R. Schwarz [a,*], U. Mardolcar [a], A. Maçarico [b], J. Martins [b], M. Vieira [b], F. Wuensch [c], M. Kunst [c], E. Morgado [d], P. Stallinga [e], H.L. Gomes [e]

[a] Departamento de Física, Instituto Superior Técnico, Lisboa, Portugal
[b] Departamento de Electrónica e Informática, Instituto Superior de Engenharia de Lisboa, Lisboa, Portugal
[c] Hahn-Meitner-Institut, Solare Energetik, Berlin, Germany
[d] Departamento de Engenharia Electrotécnica, Instituto Superior Técnico, Lisboa, Portugal
[e] Departamento de Electrotécnia, Universidade do Algarve, Faro, Portugal

Received 13 August 2007; received in revised form 16 December 2007; accepted 10 January 2008
Available online 18 January 2008

Abstract

Thick large-area particle or X-ray detectors suffer degradation during operation due to creation of defects that act as deep traps. Measuring the photocurrent under homogeneously absorbed weak light can monitor variation in detector performance. We describe how photocapacitance can be used as an alternative method to measure the creation of defects and their energy level after intense irradiation with protons or He ions at 1.5 MeV and after exposure to intense laser pulses. The possibility to detect small areas of high defect density in a large-area detector structure is discussed.

Keywords: Amorphous silicon detector; Radiation resistance; Photocapacitance

1. Introduction

As a further development of deep-level transient spectroscopy (DLTS) initiated by D.V. Lang in 1974 [1], the photocapacitance spectroscopy was introduced by the group of J.D. Cohen at the University of Oregon as an alternative to photothermal deflection spectroscopy (PDS) for the determination of the density-of-states distribution in a-Si:H thin films [2]. In contrast to PDS the transient photocapacitance technique detects the net charge change in the depletion region of the sample. Hence hole and electron transitions from gap states give signals of opposite sign.

Other authors, including Q. Wang and R.S. Crandall, applied this technique to complete p–i–n solar cells and described a combination of photocapacitance measurements, solar cell parameter measurements, combined with a computer model to show that under strong illumination photocharge increases inside the solar cell and causes field collapse and thus a decline in solar cell efficiency [3,4]. Recently, also other solar cell materials like copper indium diselenide have been studied by the photocapacitance technique [5].

For the analysis of the data presented here we have followed the derivation given by I. Nurdjaja and E.A. Schiff [6] who considered the photocapacitance C_{ph} to be a measure of the density of photogenerated carriers in the space charge region. Under low-level illumination a constant electric field across the i-layer is assumed. One then obtains the charge density ρ_{ph} which contributes to the photocapacitance C_{ph} by multiplying the average photocurrent j_{ph} with the transit time τ_T, given by [6]:

$$\tau_T = \frac{d^2}{2\mu_0 V} \qquad \text{and} \qquad \rho_{ph} = 2j_{ph}\tau_T/d. \tag{1}$$

We do not consider electrons since they are reaching the n-layer quasi instantaneously, holes are slower and correspond to the space charge ρ_{ph}. The factor 2 in the equation on the right reflects the fact that the holes need to travel

* Corresponding author. Tel.: +351-21-841 9152; fax: +351-21-841 9118.
E-mail address: rschwarz@fisica.ist.utl.pt (R. Schwarz).

0040-6090/$ - see front matter © 2008 Elsevier B.V. All rights reserved.
doi:10.1016/j.tsf.2008.01.012

only half as far (on average) to reach the collecting electrode. Finally, the photocapacitance is given by:

$$C_{\mathrm{ph}} = -\frac{d\sigma_{\mathrm{ph}}}{dV} = -d/2\frac{d\rho_{\mathrm{ph}}}{dV}. \quad (2)$$

We see that both the electric field and the transport properties of photogenerated charges, mobility and recombination lifetime, contribute to the photocapacitance signal.

Most of the experimental results we present below are measured in a 2 μm thick p–i–n detector structure (HMI-3) under different degradation conditions. We find that the photocapacitance technique can be used as an alternative to photocurrent measurements to study the defect density in both the contact regions and in the intrinsic layer.

2. Sample structure and measurement procedure

In the present work we studied two thick a-Si:H based p–i–n detectors with a 5 and 2 μm thick intrinsic layer, HMI-2 and HMI-3, respectively. The samples were deposited by plasma-enhanced chemical vapour deposition at the Hahn-Meitner-Institut (HMI) in Berlin. The relatively small contact spots of 2.2 mm diameter allowed us to analyze time-resolved photocapacitance measurements. We also studied a 3 cm × 3 cm cell structure with a thickness of 0.7 μm, IPE-1, deposited at the Institut für Physikalische Elektronik (IPE) in Stuttgart. This thickness is near to values used in solar cells, whereas particle detectors need 30–50 μm in order to assure a sufficiently high particle-induced carrier density. To compare the effect of spatial variation of photocurrent and photocapacitance we used a 1.1 μm thick and 1.5 mm × 6.8 mm large detector sample, VYG-1, prepared by Y. Vygranenko at the University of Waterloo.

We have subjected the thick detectors to a 1.5 MeV proton beam reaching a fluence of 5×10^{15} #/cm^2 at the Instituto Tecnológico e Nuclear (ITN) in Lisbon. The low stopping power of 0.1755 MeV/(mg/cm^2) assures that the protons still cross the whole detector thickness of 5 and 2 μm, respectively.

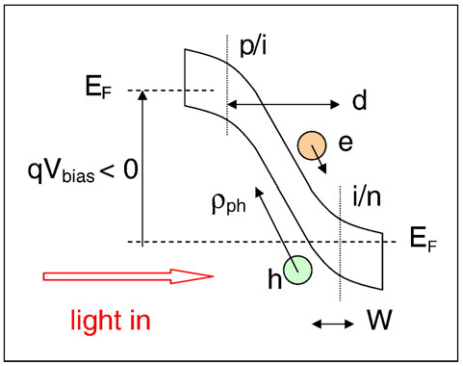

Fig. 1. Photocapacitance principle. A large reverse bias voltage V_{bias} is applied to the front p-contact of the thick p–i–n structure. Homogeneous absorption and a constant electric field are assumed. Photogenerated electrons move rapidly to the n-contact layer, whereas holes make up most of the photocharge ρ_{ph} that constitutes the photocapacitance signal according to Eq. (1). Notations: d: i-layer thickness, W: junction width of i/n interface, E_F: Fermi level, e: electron, h: hole.

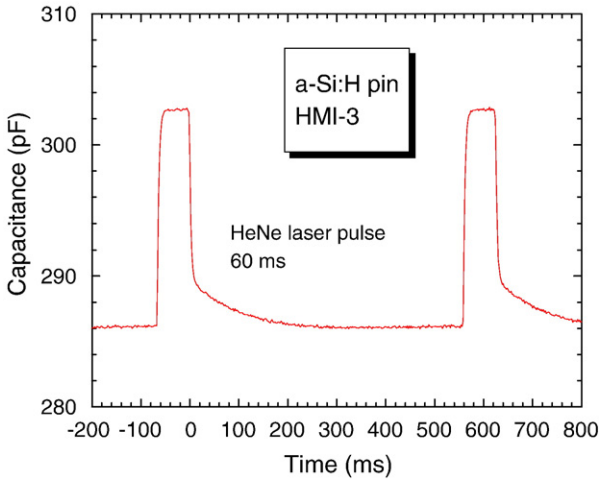

Fig. 2. Photocapacitance transients in the 2 μm thick p–i–n detector under HeNe laser pulses of 60 ms duration.

For the relatively thin detector we chose a 1.5 MeV 4He$^+$ beam with a fluence of 1.5×10^{15} ions/cm^2. Alternatively, we used 5 ns pulses from the 532 nm line of a frequency-doubled Nd:YAG laser with pulse energies at about 3 mJ/cm^2 for rapid defect creation. Before and after degradation we used the photocapacitance technique to measure the detector response.

Fig. 1 shows schematically how photogenerated holes in a thick p–i–n detector will contribute to the photocapacitance signal. Actually, three distinct regions, the junctions at the p/i and the i/n interface and the i-layer contribute to the total signal. Especially in detectors with thickness larger than a micron, the assumption of a constant electric field might not be justified. Large defect density and concomitant space charge will lead to a decay of the field with respect to the peak values at the contacts in accordance with the Poisson equation.

Experimentally, there are different ways to measure C_{ph}. For most of the measurements, especially for the capacitance transients, we used lock-in detection of the out-of-phase current through the device. Typically, we applied a sinusoidal modulation signal of 100 mV at 16 kHz and HeNe laser light modulation at 63 Hz. The voltage bias was varied between −30 V and +30 V and applied through an appropriate noise-filtering and current-limiting circuit to the sample.

3. Transient photocapacitance

Fig. 2 shows the change in capacitance of sample HMI-3 during irradiation with HeNe laser light at 633 nm. Light pulses of typically 60 ms duration and with a repetition time of 650 ms were produced with a Pockels cell operated at 120 V, and with a rise time of about 5 μs. The illumination density was about 0.3 mW/cm^2 when using a neutral density filter of ND = 1.7. The increase is about 17 pF. After the light is turned off, the capacitance does not return immediately to its base value, but shows an exponential decay as demonstrated in Fig. 3 in a semi-logarithmic plot. The characteristic decay time is 96 ms.

If we interpret this transient signal as being due to the release of photogenerated charge that is trapped at some deep level

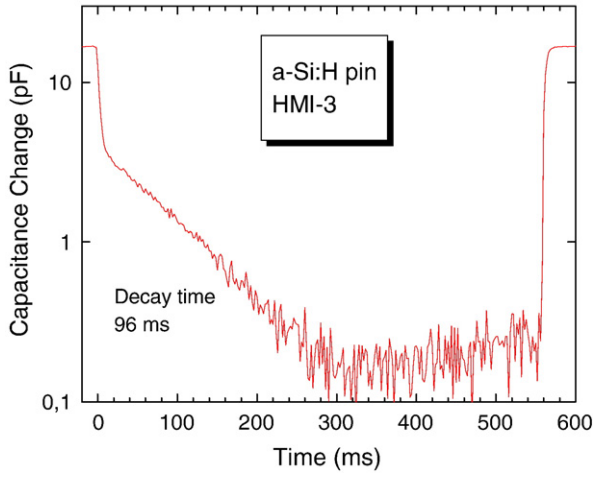

Fig. 3. Semi-logarithmic representation of the photocapacitance decay after switching off the HeNe laser. A characteristic decay time of 96 ms is measured at room temperature.

of energy E_{trap}, then by applying DLTS analysis [7,8] we can calculate this energy within a certain time window [t_1, t_2] through:

$$E_{trap} = kT \ln\left\{\frac{\ln(t_2/t_1)}{v_0 \Delta t}\right\} \quad \text{with } \Delta t = t_2 - t_1 \tag{3}$$

With kT=0.025 eV, t_2=2* t_1=200 ms, and a phonon frequency of v_0=10^{12} Hz [9] we obtain a trap depth E_{trap} of 642 meV.

An important question is the limit of operation for lock-in detection. An estimate of the transit time is 150 ns for a typical hole mobility of 0.1 cm^2/Vs in intrinsic a-Si:H, under an applied bias of −3 V. This corresponds to a limit of the detector circuit to operate at or below about 700 kHz. Above that frequency the photocapacitance signal will decrease. Here we used a modulation frequency of 16 kHz. The decay time of 96 ms (see semi-logarithmic plot in Fig. 3) is therefore not a set-up related time constant, but indeed reflects carrier release from deep traps.

We have not analyzed yet the effect of other important variables like the temperature and bias voltage which will probably change the characteristic decay time and allow to check the validity of this analysis further. We would expect, for example, the decay time to increase when lowering the measurement temperature.

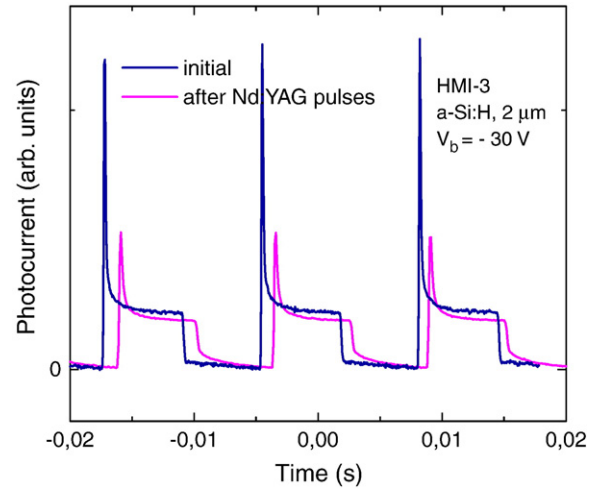

Fig. 4. Photocurrent response during illumination with HeNe laser light at 633 nm before and after degradation with Nd:YAG pulses. After degradation a slow shoulder appears in the decay after switching off the laser (see decay near −0.01 s). The curves are offset horizontally for clarity. The initial overshoot is particularly large for the non-degraded sample.

4. Degradation and photocapacitance

In a second step we have looked at the variation of photocapacitance with increasing degradation of the detector structure. We can expect different mechanisms to occur. An increase of space charge within the transition regions at the i/n and at the i/p interface would reduce the depletion layer width in those regions and therefore by definition of depletion capacitance increase the photocapacitance value. On the other hand, recombination in the intrinsic region, that is a reduction in the mobility-lifetime product of minority carriers, will reduce the photocharge σ_{ph} that constitutes the photocapacitance signal and therefore reduce its value.

Fig. 4 shows the photocurrent pulses that are monitored before and after degradation of sample HMI-3 by strong Nd:YAG laser pulses. Different effects are seen. The onset of the HeNe laser induced photocurrent shows a strong overshoot indicative of a capacitive component of the device. After switching off the light, the photocurrent returns rapidly to the initial value in the non-degraded case, but shows again a slow shoulder after degradation. We are interested to compare the reduction in the stabilized photocurrent level with the change of photocapacitance for the same situation.

Fig. 5 shows that indeed both the average photocurrent and the magnitude of photocapacitance decrease by the same amount of ca. 32%.

Finally, we compared two scans of the modulated HeNe laser across the 1.1 µm thick detector VYG-1 previously irradiated with $4He^+$ ions, monitoring both the photocurrent and the local

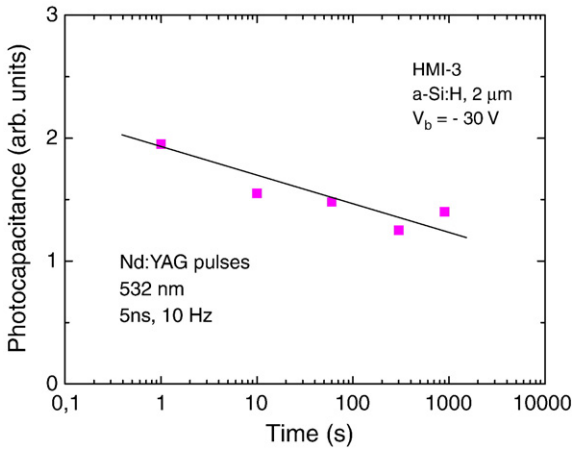

Fig. 5. Photocapacitance signal as a function of sample irradiation with short Nd:YAG laser pulses.

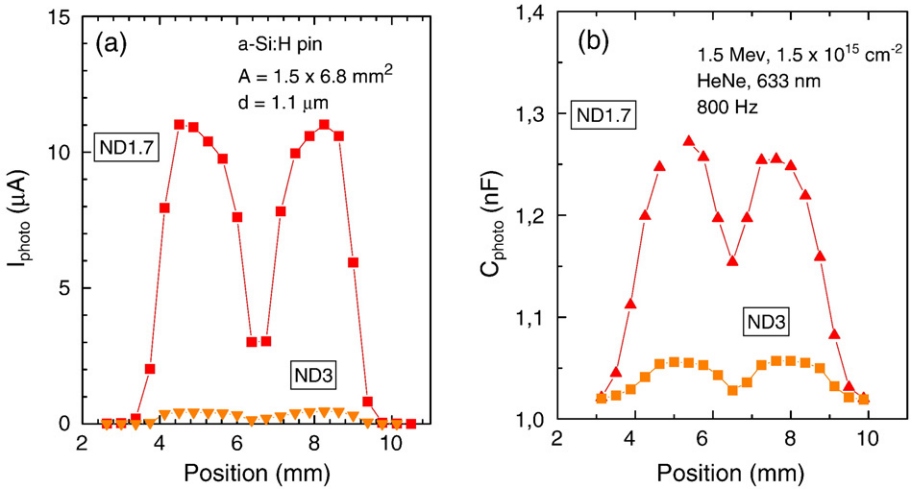

Fig. 6. a-Si:H pin detector VYG-1 of 1.1 μm thickness irradiated by 1.5 MeV $4He^+$ ions with accumulated fluence of 1.5×10^{15} cm^{-2}. (a) Photocurrent scan across the 6.8 mm long sample. (b) Photocapacitance signal across the same region. ND denotes the strength of the neutral density filters to attenuate the HeNe laser beam used for readout.

photocapacitance, as shown in Fig. 6(a) and (b), respectively. The central degraded area is evident in both scans.

5. Discussion

From the previous two figures we conclude that photocapacitance is sensitive to the reduction of the transport parameters in the active layer of the detector structure. Under HeNe laser illumination we find a positive photocapacitance signal consistent with both a reduction in space charge width at the interfaces and with the contribution of photocharge created inside the intrinsic layer.

The transient photocapacitance analysis leads to a trap depth of about 0.64 eV, which might be attributed to a hole trap state above the valence band. The contribution of the contact layers is not dominant in the measurement of degradation consistent with the geometrical parameters of a thick detector.

We have not seen any appreciable effect in the 5 μm thick sample HMI-2. This is probably due to the limited collection probability of photocharge. Carriers are recombining before they reach the contacts, consistent with the particular shape of the spectral response that is strongly peaked near the band gap of 1.7 eV of a-Si:H. On the other hand, in a thick detector structure, the electric field will be quenched in the center of the sample, in contradiction to the assumptions made above for the definition of photocapacitance.

We were unable to detect the expected decrease in photocapacitance signal after laser degradation of the 3×3 cm^2 sample IPE-1. The reason lies in the large (dark) capacitance of about 130 nF of this detector. The photocapacitance signal was about 10.000 times smaller. The change in photocapacitance lies then even below this value, and was below the resolution of the time-resolved photocapacitance measurement set-up which we used.

The photocapacitance scans in the sample VYG-1 in Fig. 6 prove that this is a valid alternative to photocurrent scans when monitoring local film degradation of thin p–i–n detectors. We note, however, a difference to the roughly inversely linear dependence of photocurrent with defect density. In the case of photocapacitance the signal is strongly sublinear with HeNe laser light intensity.

6. Summary

We have tested a-Si:H based p–i–n detector structures of various thicknesses to monitor the photocapacitance signal in both the as-deposited and the degraded state after 1.5 MeV proton or $4He^+$ ion irradiation. The transient photocapacitance measurements can be explained by reemission of photogenerated charge from 0.64 eV deep trap levels, presumably hole traps above the valence band. We compared the decrease in photocurrent and photocapacitance level after fast degradation generated by strong Nd:YAG laser pulses. Both measurements yield a similar relative change. This is consistent with the model of sensitivity of photocapacitance to the transport properties of photogenerated charge in the thick intrinsic layer.

Acknowledgements

We want to thank M. Schubert and Y. Vygranenko for supplying detector samples, and C.P. Marques and E. Alves for particle irradiation runs at ITN. The work at IST, ISEL, and University of Algarve is supported by Fundação para a Ciência e a Tecnologia (FCT) through project POCTI/FP/FNU/50352/2003 (MSIC-2).

References

[1] D.V. Lang, J. Appl. Phys. 45 (1974) 3023.
[2] A.V. Gelatos, J.D. Cohen, J.P. Harbison, Appl. Phys. Lett. 49 (1986) 772.
[3] R.S. Crandall, Appl. Phys. Lett. 42 (1983) 451.
[4] Q. Wang, R.S. Crandall, E.A. Schiff, Proceedings of the 21st Photovoltaics Specialists Conference, IEEE, 1996, p. 1113.
[5] M. Igalson, A. Urbaniak, Bull. Polish Acad. Sci. 53 (2005) 157.
[6] I. Nurdjaja, E.A. Schiff, Mater. Res. Soc. Symp. Proc. 467 (1997) 723.
[7] R. Schwarz, J.J. Sun, R. Rocha, E. Morgado, P.P. Freitas, Mater. Sci. Forum 258 (1997) 1259.
[8] D.K. Schroeder, Semiconductor Material and Device Characterization, John Wiley & Sons, New York, 1990.
[9] D. Monroe, Phys. Rev. Lett. 54 (1985) 146.